Original Article

Impact of Molecular Imaging on the Diagnosis of Dementia Subtypes

Chetsadaporn Promteangtrong MD[1], Chanikarn Poenateetai MD, BSc[1], Aattapon Jantarato BSc[1], Nathapol Boonsingma BSc[1], Anchisa Kunawudhi MD[1], Chanisa Chotipanich MD[1]

[1] National Cyclotron and PET Centre, Chulabhorn Hospital, Chulabhorn Royal Academy, Bangkok, Thailand

Objective: To evaluate the impact of positron emission tomography with ^{18}F-FDG, ^{11}C-PiB, and ^{18}F-THK 5351 on the diagnosis of Alzheimer's disease, primary tauopathies, and other dementia subtypes.

Materials and Methods: The authors recruited 30 patients with varying degrees of cognitive impairment that included 14 males and 16 females, aged 50 to 77 years and with a mean age ±SD: 66.6±6.9 years). All patients underwent ^{18}F-FDG, ^{11}C-PiB, and ^{18}F-THK 5351 PET/CT scans. Quantitative and visual analyses of the PET images were performed and reported back to the neurologists responsible for the initial diagnoses. Outcome measures were changed between pre- and post-PET clinical diagnoses and treatment.

Results: The primary diagnoses changed after the disclosure of ^{18}F-FDG, ^{11}C-PiB, and ^{18}F-THK 5351 PET scan results in 18 of 30 patients (60%) and was able to resolve 20 of 21 (95.2%) pre-PET diagnostic dilemmas. No new diagnostic dilemmas were created. All changes in clinical diagnoses were accompanied by changes in treatment plan. PET imaging results confirmed the initial diagnoses of six patients.

Conclusion: Combined ^{11}C-PiB, ^{18}F-THK 5351, and ^{18}F-FDG-PET are of additional diagnostic value over standard diagnostic work-up, especially in diagnostic dilemmas or difficult-to-diagnose dementia patients.

Keywords: ^{18}F-FDG; ^{11}C-PiB; ^{18}F-THK 5351; Positron emission tomography; Tauopathy

Received 26 October 2020 | Revised 20 August 2021 | Accepted 23 August 2021

J Med Assoc Thai 2021;104(12):1873-80

Website: http://www.jmatonline.com

With the rapid aging of the world's population, the prevalence of dementia is continually on the rise. In 2015, the number of people suffering from dementia worldwide was estimated at 47.47 million. This is expected to reach 75.63 million in 2030 and 135.46 million in 2050[1]. In Thailand, the prevalence of dementia was reported to be 2% to 10% of the Thai population, with 70% attributing to Alzheimer's disease (AD)[2]. Other commonly encountered disorders include frontotemporal dementia (FTD), Parkinson's disease without (PD) and with later dementia (PDD), dementia with Lewy bodies (DLB), progressive supranuclear palsy (PSP), and corticobasal degeneration (CBD). It is important to correctly distinguish between these disorders as this allows for timely implementation of disease-specific treatment. However, the current clinical diagnostic guidelines for various subtypes of dementia are limited in terms of sensitivity and specificity[3]. To date, definitive diagnosis of these neurodegenerative disorders can only be established with histopathological analysis, which is obtained only after autopsy of biopsy[4].

There are advances in molecular neuroimaging modalities such as amyloid pathological imaging with carbon-11-labelled Pittsburgh compound B (^{11}C-PiB) positron emission tomography (PET), Tau pathological imaging with ^{18}F-THK-5351 PET, and functional imaging with [^{18}F]-2-fluoro-2-deoxy-D-glucose (^{18}F-FDG) PET. Then, as those modalities become more popular, they are used in routine clinical practice to aid in the diagnosis of dementia subtypes. The ^{18}F-FDG is the more established radiotracer and considered a marker of neurodegeneration, most specifically of synaptic loss[5]. The ^{18}F-FDG does not directly measure neuropathology, but the extent of altered glucose metabolism predicts the degree of cognitive impairment and is strongly correlated with disease severity[6]. The ^{18}F-FDG PET has high sensitivity (94%), but low specificity

Correspondence to:

Chotipanich C.

National Cyclotron and PET Centre, Chulabhorn Hospital, Chulabhorn Royal Academy, 906 Kamphaeng Phet 6 Road., Talat Bang Khen, Lak Si, Bangkok 10210, Thailand.

Phone: +66-2-5743355 ext. 1211

Email: chanisa.cho@pccms.ac.th

How to cite this article:

Promteangtrong C, Poenateetai C, Jantarato A, Boonsingma N, Kunawudhi A, Chotipanich C. Impact of Molecular Imaging on the Diagnosis of Dementia Subtypes. J Med Assoc Thai 2021;104:1873-80.

doi.org/10.35755/jmedassocthai.2021.12.12161

(73%) for distinguishing between AD and other neurodegenerative disorders, as metabolic patterns may overlap[7]. β-amyloid (Aβ) plaques and tau neurofibrillary tangles (NFT) are the hallmark pathologies of AD. Aβ plaque deposition usually begins decades before the onset of symptoms, while tau aggregation is strongly associated with neurodegeneration and cognitive deficits[8]. Thus, making tau imaging a more suitable marker of disease progression. Radiotracers with high affinity to Aβ plaques and tau proteins have been employed for human PET imaging. The ^{11}C-PiB binds to fibrillar Aβ, which allows the in vivo detection of Aβ plaques and the ability to distinguish between AD and other non-AD dementia. The specificity and sensitivity of ^{11}C-PiB PET in distinguishing between AD and FTD was 89% and 84%, respectively[9]. More recently, the development of tau-specific ligands with PET has now made it possible to investigate tau deposition patterns in neurodegenerative disease. The ^{18}F-labeled arylquinoline derivative, ^{18}F-THK-5351, demonstrated selective and high binding affinity for tau over Aβ, as well as increased tracer uptake at the sites of tau pathology in AD[10,11]. It is also important to note that besides AD, abnormal accumulation of tau protein is observed in a variety of other neurodegenerative disorders, termed primary tauopathies[12]. They may be composed of different tau isoforms and have distinct distribution patterns in the brain. Tau PET imaging can potentially assist in the accurate and early differential diagnosis of these non-AD tauopathies. Combined, these radiotracers allow the differentiation of AD, non-AD tauopathies, and other dementias that may present as diagnostic challenges, especially in their initial stages, as symptoms are often non-specific.

The aim of the present study was to evaluate the impact of combined ^{18}F-FDG, ^{11}C-PiB, and ^{18}F-THK-5351 PET on the diagnoses of AD, primary tauopathies, and other dementia subtypes.

Materials and Methods

The prospective study was approved by the Human Research Ethics Committee of the authors' institute on December 23, 2016, Project code was 043/2559. Before commencing the study, written informed consents were obtained from all subjects for participation in the present study of data for research and educational purposes.

Subjects and diagnostic procedure

The authors identified 30 patients with varying degrees of cognitive impairment that included 14 males and 16 females, aged 50 to 77 years, with a mean age ±SD: 66.6±6.9 years who had undergone ^{18}F-FDG, ^{11}C-PiB, and ^{18}F-THK 5351 PET scans between 2016 and 2017, and had been assessed clinically before and after the scans. All participants underwent standard dementia diagnostic work-up consisting of comprehensive medical and neurological evaluation, screening laboratory tests, and brain magnetic resonance imaging (MRI). None was clinical depressed, had other psychiatric illnesses, or history of psychotropic drug use at the time of the study. Each participant underwent cognitive evaluation that included the Montreal Cognitive Assessment (MoCA) or the Thai Mental State Examination (TMSE). This was followed by ^{18}F-FDG, ^{11}C-PiB, and ^{18}F-THK 5351 PET scans using a Siemens/Biograph 16 scanner in 3D mode. All scans were performed within two weeks of the baseline screening visit.

MRI acquisition

T1-weighted MRI was acquired in all participants for registration and delineation of the brain reference regions using PMOD Neuro tool (PMOD Technologies, Zürich, Switzerland)[13,14]. Additional sequences of MRI such as Diffuse weight images (DWI), Fluid-attenuated inversion recovery (FLAIR), and T2-weighted MRI (T2W) were used for detecting other underlying intracranial pathologies.

^{18}F-FDG PET imaging procedure

All participants fasted for six hours before being scanned using a Siemens/Biograph 16 scanner in 3D mode. Plasma glucose levels were measured before the ^{18}F-FDG PET/CT scan, with acceptable levels being less than 200 mg/dL. Imaging was then performed 50 minutes after intravenous injection of 5 MBq/kg ^{18}F-FDG. Image acquisition was performed for 10 minutes per bed position, matrix size=256×256, zoom=1, and a Gaussian filter of FWHM=2.0. Image reconstruction was performed using the ordered subset expectation maximization (OSEM) with four iterations and eight subsets.

^{11}C-PiB imaging procedure

All participants were scanned using a Siemens/Biograph 16 scanner in 3D mode. Dynamic imaging was performed immediately after intravenous injection of 555 MBq (15 mCi) of ^{11}C-PiB. Dynamic brain PET/CT scanning was performed for 70 minutes, and brain CT images were also acquired for attenuation correction. The image acquisition used a

matrix size of 168, zoom of 1, and a Gaussian filter with a full-width at half-maximum (FWHM) of 5.0. Images were reconstructed into seven frames of 10 minutes per frame, using ordered subset expectation maximization (OSEM) with four iterations, eight subsets, and a 4-mm pixel size. The iterative reconstruction images from 50 to 70 minutes were used for quantitative analysis.

^{18}F-THK 5351 imaging procedure

Dynamic imaging was performed immediately after intravenous injection of 185 MBq (5 mCi) of ^{18}F-THK 5351. Dynamic brain PET/CT scanning was performed for 90 minutes and brain CT images for attenuation correction were also acquired. The image acquisition used a matrix size of 168, zoom of 1, and a Gaussian filter with a FWHM of 5.0. Images were reconstructed into four frames of 20 minutes per frame using ordered subset expectation maximization (OSEM) with four iterations, eight subsets, and a 4-mm pixel size. The iterative reconstruction images from 40 to 60 minutes were used for quantitative analysis.

PET imaging analysis

Quantitative analysis: PET imaging data was processed and analyzed using P-mod Neuro tool (PMOD Technologies). Both ^{11}C-PiB and ^{18}F-THK-5351 PET images were automatically co-registered within individuals using an automatic voxel of interest method. Both the ^{11}C-PiB and ^{18}F-THK-5351 PET images were automatically co-registered to individual T1-weighting MRI images. Then, the SUVRs of ^{11}C-PiB and ^{18}F-THK 5351 in various cortical regions were analyzed, using the cerebellum as a reference region. The eight ^{11}C-PiB regions included orbitofrontal, precuneus, parietal, anterior cingulate, posterior cingulate, superior parietal, lateral temporal, and occipital areas. The ^{18}F-THK-5351 regions were the anterior cingulate, brain stem, caudate nucleus, white matter, entorhinal cortex, frontal cortex, fusiform gyrus, hippocampus, inferior temporal cortex, lingual gyrus, middle temporal gyrus, occipital cortex, pallidum, parahippocampal gyrus, parietal cortex, posterior cingulate, precuneus, putamen, and thalamus.

Visual analysis: The ^{18}F-FDG, ^{11}C-PiB, and ^{18}F-THK 5351 PET scans were visually rated by an experienced nuclear medicine physician. The ^{18}F-FDG scans were interpreted as either normal or AD as hypometabolism involving the temporoparietal cortex, posterior cingulate cortex, and precuneus, FTD as frontotemporal hypometabolism, DLB as occipital hypometabolism with intact posterior cingulate cortex, PSP as frontal, basal ganglia, and midbrain hypometabolism, or CBD as asymmetrical hypometabolism involving the parietal, central, frontal cortex, striatum, and thalamus. ^{11}C-PiB PET scans were rated as either positive or negative for cortical ^{11}C-PiB. A positive scan was defined as having significantly greater ^{11}C-PiB uptake in the cortical region than in white matter. On the other hand, a negative scan was defined as having white matter ^{11}C-PiB binding. ^{18}F-THK 5351 PET scans were interpreted based on the extent of ^{18}F-THK 5351 uptake at inferior temporal cortex, midbrain, medulla, pons, and precuneus using the cerebellar grey matter as a reference region.

Data analysis: Based on clinical manifestations and neuropsychological tests, the initial pre-PET diagnoses were divided into "AD" or "non-AD" categories. AD diagnoses included both typical and atypical presentations of AD such as early onset AD, late onset AD, MCI due to AD, and DLB with AD. The non-AD category consisted of clinical subgroups of FTLD, PSP, CBD, chronic traumatic encephalopathy (CTE), and others dementia. In the cases with multiple differential diagnoses, the first diagnosis listed was considered "primary" and patients were further classified as "diagnostic dilemmas". All participants had ^{18}F-FDG, ^{11}C-PiB, and ^{18}F-THK 5351 PET scans within two weeks. Results were disclosed and then reported back to the treating physician, who recorded a revised clinical diagnosis and treatment plan considering the PET imaging results along with all other information. The initial diagnosis and intended management at baseline were compared to those obtained after receiving the PET scan results to assess for changes. Continuous variables were presented as mean ± standard deviation (SD). Summary and descriptive statistics analysis were used. Stata, version 11 (StataCorp LP, College Station, TX, USA) was applied for all analyses.

Results

Pre-PET demographics and diagnoses

After initial standard dementia work-up, 43.3% of patients were given a diagnosis of AD and the remaining 56.7% had a non-AD etiologic diagnosis. Seventy percent of patients were also classified as diagnostic dilemmas, as they had multiple differential diagnoses. Amongst patients with an AD etiologic diagnosis, 61.5% had a diagnosis of early onset AD, 23.1% had a diagnosis of late onset AD, and 15.4%

Table 1. Clinical and demographic characteristics (total n=30)

Age at PET (year); mean±SD	66.6±6.9
Sex; n	
Male	14
Female	16
Years of education (year); mean±SD	11.9±5.2
Handedness; n	
Right	28
Left	2
MoCA (score); mean±SD	16.4±6.1
Diagnostic dilemmas; n	21
Primary clinical diagnosis; n	
AD	13
Non-AD	17
Pre-PET clinical diagnosis; n	
AD	13
Non-AD	17
• FTLD	7
• CBD	3
• PSP	3
• CTE	2
• DLB	2

PET=positron emission tomography; MoCA=Montreal Cognitive Assessment; AD=Alzheimer's disease; FTLD=frontotemporal lobar degeneration; CBD=corticobasal degeneration; PSP=progressive supranuclear palsy; CTE=chronic traumatic encephalopathy; DLB=dementia with Lewy bodies; SD=standard deviation

had MCI due to AD. Amongst patients with a non-AD diagnosis, the most common diagnosis was FTLD (41.1%), followed by PSP (23.5%), CBD (23.5%), CTE (11.8%), and DLB (11.8%). Patients in the FTLD category included diagnoses of behavioral variant FTD (bvFTD) (71.4%), progressive non-fluent aphasia (PNFA) (14.3%), and semantic dementia (SD) (14.3%). Demographical data and clinic characteristics are summarized in Table 1.

PET-scan results

Ninety-six-point-seven percent of patients had a positive ^{18}F-FDG PET scan (n=29) and 3.3% (n=1) had a negative scan. The ^{11}C-PiB PET scan was positive in 63.3% of patients (n=19) and negative in 36.7% (n=11). The ^{18}F-THK 5351 PET was positive in 76.7% of patients (n=23) and negative in 23.3% (n=7). Approximately 77% of patients with a pre-PET diagnosis of AD had a positive ^{11}C-PiB PET scan, while 84.6% had a positive ^{18}F-THK 5351 PET scan. Amongst patients with a pre-PET diagnosis of non-AD etiology, 58.8% had a positive ^{11}C-PiB PET scan and 70.6% had a positive ^{18}F-THK 5351 PET scan.

Diagnostic changes

The primary diagnosis changed after the disclosure of ^{18}F-FDG, ^{11}C-PiB, and ^{18}F-THK 5351 PET scan results in 18 patients (60%). Six patients initially diagnosed with FTLD were reclassified, making it the group in which most patients were reclassified. Four patients were reclassified to AD, one patient to CTE, one patient to PSP, and only one patient remained FTLD. This was followed by the AD group with two patients reclassified to primary age-related tauopathy (PART), and two patients to suspected non-Alzheimer pathophysiology (SNAP). An initial diagnosis of CBD (n=3) remained CBD in one patient, while the rest was changed to either FTLD or PSP. In patients with an initial diagnosis of PSP (n=3), the post-PET diagnosis remained PSP in one patient, while the rest was changed to either vascular dementia or multiple system atrophy (MSA). Additionally, four patients were reclassified from the CTE and DLB group to AD. PET scan results and clinical outcome are summarized in Table 2. All changes in clinical diagnoses were accompanied by changes in treatment plan. Following the disclosure of PET scan results, the number of diagnostic dilemmas decreased from 21 to 1, with the resolution of 20 pre-PET dilemmas. No new diagnostic dilemmas were created. Initial diagnoses were confirmed with PET scan results in six patients, all of which were AD.

Example cases

Case number 4: A 58-year-old female presented with visual dysfunction, amnesia, and dyscalculia. MOCA and TMSE were eight and 20, respectively. Initial diagnosis was early onset AD. The ^{18}F-FDG, ^{11}C-PiB, and ^{18}F-THK 5351 PET scans are shown in Figure 1. Final diagnosis was AD and molecular imaging results confirmed the initial diagnosis.

Case number 18: A 65-year-old female presented with disinhibition, parkinsonism, and vertical gaze paresis. MOCA and TMSE were 12 and 24, respectively. Initial diagnosis was PSP and differential diagnosis was AD with corticobasal syndrome. ^{18}F-FDG, ^{11}C-PiB, and ^{18}F-THK 5351 PET scans are shown in Figure 2. Final diagnosis was PSP and molecular imaging results resolved the diagnostic dilemma.

Case number 21: A 70-year-old female presented with spastic left hemiparesis, recurrent falls, and irritability. MOCA was 21. Initial diagnosis was CBD and differential diagnosis was PSP. ^{18}F-FDG, ^{11}C-PiB,

Table 2. PET scan results and clinical outcomes

Patient No.	Age (years)	Sex	PET results			Initial diagnosis	Final diagnosis
			^{18}F-FDG	^{11}C-PiB	^{18}F-THK 5351		
1	63	F	Positive	Positive	Positive	FTD	AD
2	67	M	Positive	Positive	Positive	AD	AD
3	57	F	Positive	Positive	Positive	AD	AD
4	58	F	Positive	Positive	Positive	AD	AD
5	63	M	Positive	Positive	Positive	AD	AD
6	77	M	Positive	Positive	Positive	FTD	AD
7	68	F	Positive	Positive	Positive	DLB	AD
8	73	F	Positive	Positive	Positive	FTD	AD
9	71	F	Positive	Positive	Positive	AD	AD
10	70	M	Positive	Positive	Positive	AD	AD
11	69	F	Positive	Positive	Positive	CTE	AD
12	69	M	Positive	Positive	Positive	CTE	AD
13	70	F	Positive	Positive	Positive	AD	AD
14	53	F	Positive	Positive	Positive	AD	AD
15	50	F	Positive	Positive	Negative	FTD	AD
16	67	M	Positive	Positive	Positive	DLB	AD
17	60	F	Positive	Negative	Positive	CBD	PSP
18	65	F	Positive	Negative	Positive	PSP	PSP
19	64	M	Positive	Negative	Positive	FTD	CTE
20	63	M	Positive	Negative	Negative	FTD	FTD
21	70	F	Positive	Negative	Negative	CBD	FTD
22	69	M	Positive	Negative	Positive	FTD	PSP
23	75	M	Positive	Positive	Negative	PSP	MSA
24	77	M	Positive	Negative	Negative	PSP	VaD
25	68	F	Positive	Negative	Positive	CBD	CBD
26	74	F	Positive	Positive	Negative	AD	PART
27	76	M	Positive	Negative	Negative	AD	PART
28	55	M	Positive	Positive	Positive	AD	AD
29	68	F	Positive	Negative	Positive	AD	SNAP
30	69	M	Positive	Negative	Positive	AD	SNAP

PET=positron emission tomography; F=female; M=male; AD=Alzheimer's disease; DLB=dementia with Lewy bodies; FTD=frontotemporal dementia; PSP=progressive supranuclear palsy; CBD=corticobasal degeneration; CTE=chronic traumatic encephalopathy; MSA=multiple system atrophy; VaD=vascular dementia; PART=primary age-related tauopathy; SNAP=suspected non-Alzheimer pathophysiology

and ^{18}F-THK 5351 PET scans are shown in Figure 3. Final diagnosis was FTD and molecular imaging results changed the diagnosis and treatment planning.

Discussion

The primary aim of the present study was to assess the impact of amyloid and tau PET imaging on diagnostic process and clinical decision making in dementia patients. The present study findings suggest that molecular imaging is of additional value over standard diagnostic work-up, given that 60% of the initial clinical diagnoses changed after PET. This is, to the authors' knowledge, the first study to examine added diagnostic value of ^{11}C-PiB in conjunction with ^{18}F-THK 5351 and ^{18}F-FDG-PET. However, a previous study on ^{11}C-PiB and ^{18}F-FDG-PET have reported a lower percentage of diagnostic changes (23%)[6]. Altomare et al had studied the changes of diagnosis and diagnostic confidence of amyloid PET and ^{18}F-Flortaucipir tau PET, both individually and in combination, in an unselected memory clinic population. They reported a change of etiological

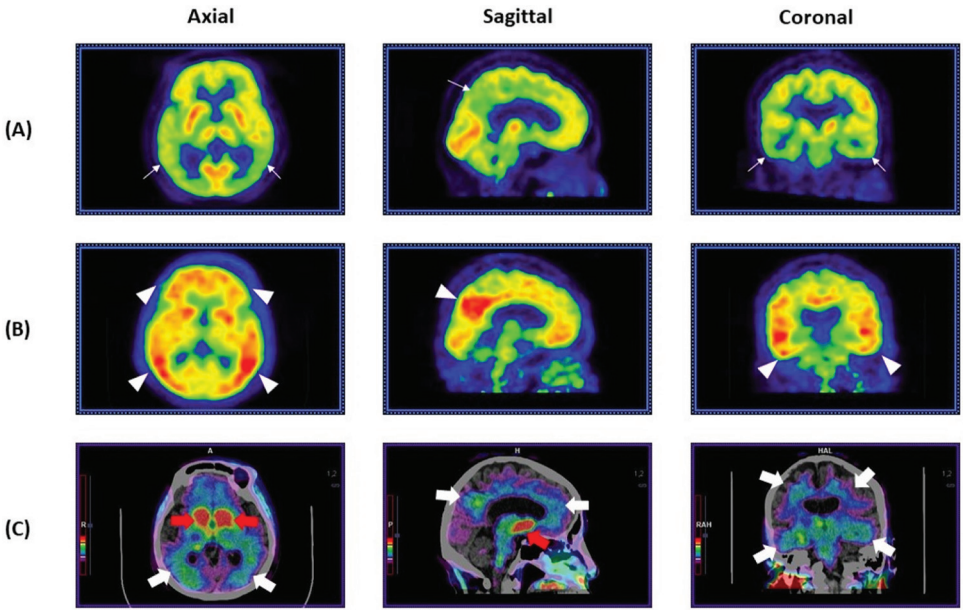

Figure 1. (A) ^{18}F-FDG PET showed hypometabolism at bilateral parieto-temporo-occipital regions including precuneus and posterior cingulated gyri (white line arrow). (B) ^{11}C-PiB PET showed diffusely increased tracer uptake at whole neocortical brain (white arrowhead) with SUVR=2.19. (C) ^{18}F-THK 5351 PET with CT fusion showed increased tracer uptake at frontal (SUVR=1.57), parietal (SUVR=1.45), temporal (SUVR=1.68) and occipital (SUVR=1.53) regions (white block arrow). Intense 18F-THK 5351 uptake at bilateral basal ganglia and thalamus was noted as off-target binding (red block arrow). PET data were interpreted as AD.

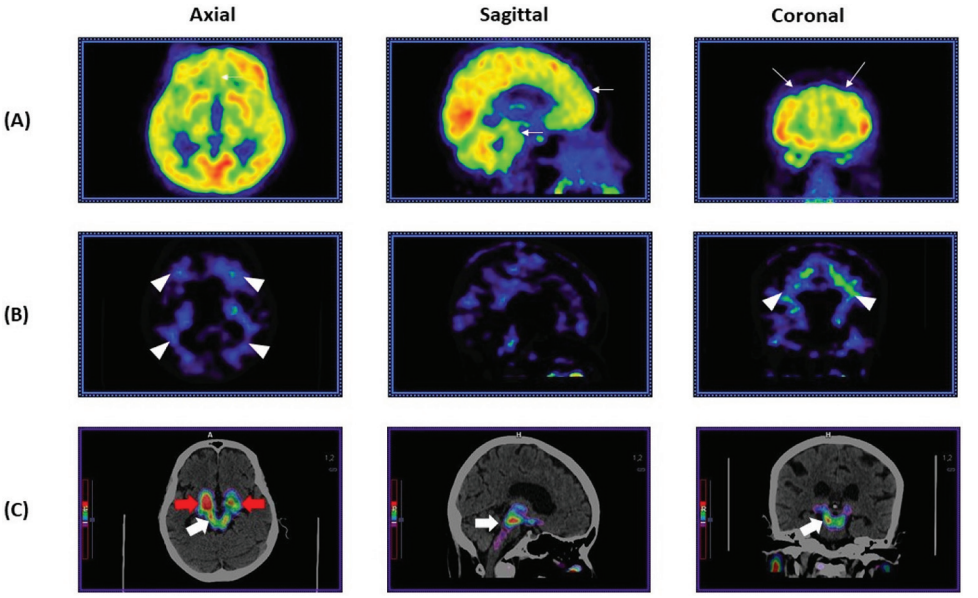

Figure 2. (A) ^{18}F-FDG PET showed hypometabolism at dorsolateral frontal lobes, medial frontal lobes, and midbrain (white line arrow). (B) ^{11}C-PiB PET showed no abnormal tracer uptake at neocortical brain with normal physiologic uptake at white matter (white arrowhead) correlated with SUVR=0.55. (C) ^{18}F-THK 5351 PET with CT fusion showed increased tracer uptake at midbrain (SUVR=2.87) (white block arrow). ^{18}F-THK 5351 uptake at bilateral basal ganglia as off-target binding was noted (red block arrow). PET data were interpreted as PSP.

diagnosis in 28% after individual amyloid PET or tau PET when presented as the first exam while the diagnostic change after the second exam was less than 10% for both PET imaging. Significant and similar

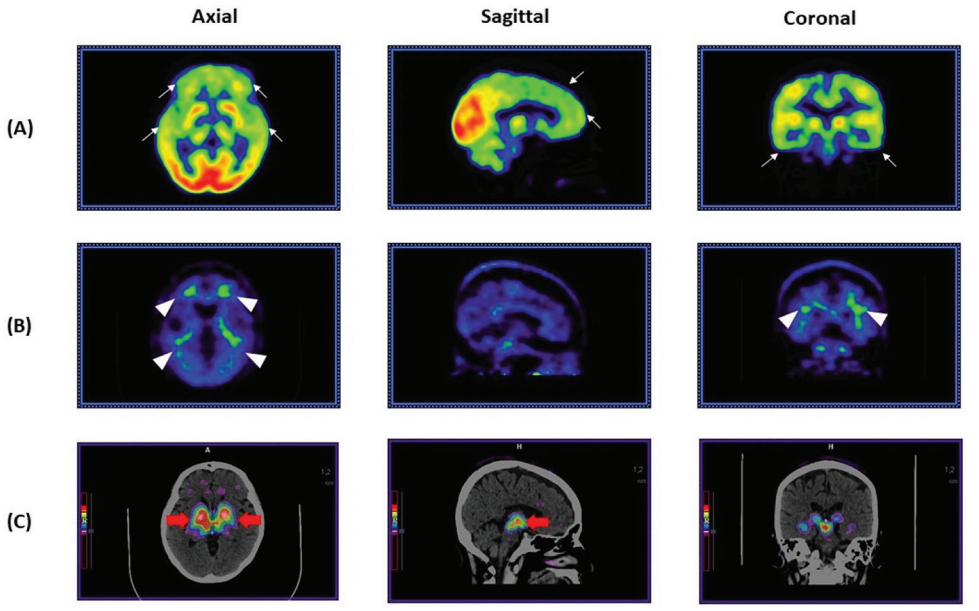

Figure 3. (A) ^{18}F-FDG PET showed hypometabolism at bilateral frontal lobes and mild hypometabolism at bilateral temporal lobes (white line arrow). (B) ^{11}C-PiB PET showed no abnormal tracer uptake at neocortical brain with normal physiologic uptake at white matter (white arrowhead) correlated with SUVR=1.00. (C) ^{18}F-THK 5351 PET with CT fusion showed no abnormal tracer uptake in cortical brain with off-target binding at bilateral basal ganglia and thalamus (red block arrow). PET data were interpreted as FTD.

increases in diagnostic confidence due to amyloid PET or tau PET were also observed[15]. However, Altomare et al may be limited by the retrospective nature with no ^{18}F-FDG-PET and they interpreted PET scans only as AD or non-AD, while the present study was prospective and categorized non-AD group in term of various diseases. Seventy percent of patients in the present study met the criteria for "diagnostic dilemma". This is due to the study population consisting of difficult cases that clinicians felt reluctant to assign a higher probability to one of the multiple differential diagnoses listed. The disclosure of PET results was able to resolve 95.2% of these diagnostic dilemmas, demonstrating that clinicians were able to identify a subset of patients in whom amyloid and tau PET will be most clinically beneficial.

The present study was descriptive and has limitations. First, this was a preliminary study with a small sample size that may not fully represent all variants of dementia. The authors also were not able to assess the effect of PET on the diagnostic confidence of clinicians. Because of this, the authors also cannot separate the influence of tau, amyloid, and FDG PET on the diagnostic process. This information may additionally guide the most suitable modality of molecular imaging for individual selected patient in routine clinical practice, which may be more cost-benefit than performing all three tracers. Furthermore, this was an uncontrolled study, whereas a randomized controlled design would have given a more accurate estimation of the clinical utility of PET. This would also allow for direct comparison with other diagnostic biomarkers. Moreover, the single center design limits the generalizability of the findings, particularly to less specialized clinical settings. Further studies are needed to validate post-PET scan diagnoses, their implications on long-term treatment planning, as well as cost-effectiveness.

Conclusion

The present study findings support an additive value of ^{18}F-FDG, ^{11}C-PiB, and ^{18}F-THK 5351 PET imaging to dementia diagnostic work-up, especially in cases with atypical presentation, diagnostic dilemmas, or difficult-to-diagnose dementia patients. Combined ^{18}F-FDG, ^{11}C-PiB, and ^{18}F-THK 5351 PET imaging changed the final diagnoses in 60% of cases and was able to resolve 95.2% of all diagnostic dilemmas. This has impact on clinical diagnosis and patient management planning. In these patients, an accurate diagnosis can help direct therapy, improve care plan, and avoid unnecessary drug prescription. The present study results provide additional evidence for future recommendations regarding the use of brain PET imaging in clinical practice.

Acknowledgement

The authors would like to extend a special thanks to Chulabhorn Hospital, Chulabhorn Royal Academy for the funding support. The authors also convey their grateful thanks to Dr. Jintana Assanasen for clinical and neuropsychological information. Additionally, special gratitude is extended to Professor Shozo Furumoto, University of Tohoku, Sendai, Japan, for the provision of THK precursor in the study. Finally, the authors very much appreciated Professor Eyal Mishani, PhD, Director of Cyclotron/Radiochemistry Unit, Department of Nuclear Medicine, Hadassah Medical Center, Israel, as the visiting professor and consultant for the authors radiotracer production at the authors National Cyclotron and PET Centre, Chulabhorn Hospital, Chulabhorn Royal Academy, Bangkok, Thailand.

Conflict of interest

All authors declare no personal or professional conflicts of interest.

References

1. World Health Organization. The epidemiology and impact of dementia: Current state and future trends. Report No.: WHO/MSD/MER/15.3 [Internet]. 2015 [cited 2015 Jun 23]. Available from: https://www.who.int/mental_health/neurology/dementia/dementia_thematicbrief_epidemiology.pdf.
2. Sittironnarit G, Emprasertsuk W, Wannasewok K. Quality of life and subjective burden of primary dementia caregivers in Bangkok, Thailand. Asian J Psychiatr 2020;48:101913.
3. Shea YF, Ha J, Lee SC, Chu LW. Impact of (18) FDG PET and (11)C-PIB PET brain imaging on the diagnosis of Alzheimer's disease and other dementias in a regional memory clinic in Hong Kong. Hong Kong Med J 2016;22:327-33.
4. James OG, Doraiswamy PM, Borges-Neto S. PET Imaging of Tau Pathology in Alzheimer's Disease and Tauopathies. Front Neurol 2015;6:38.
5. Banzo I, Jiménez-Bonilla J, Ortega-Nava F, Quirce R, Martínez-Rodríguez I, de Arcocha-Torres M, et al. Amyloid imaging with (11)C-PIB PET/CT and glucose metabolism with (18)F-FDG PET/CT in a study on cognitive impairment in the clinical setting. Nucl Med Commun 2014;35:238-44.
6. Ossenkoppele R, Prins ND, Pijnenburg YA, Lemstra AW, van der Flier WM, Adriaanse SF, et al. Impact of molecular imaging on the diagnostic process in a memory clinic. Alzheimers Dement 2013;9:414-21.
7. Davison CM, O'Brien JT. A comparison of FDG-PET and blood flow SPECT in the diagnosis of neurodegenerative dementias: a systematic review. Int J Geriatr Psychiatry 2014;29:551-61.
8. Dani M, Brooks DJ, Edison P. Tau imaging in neurodegenerative diseases. Eur J Nucl Med Mol Imaging 2016;43:1139-50.
9. Vandenberghe R, Adamczuk K, Dupont P, Laere KV, Chételat G. Amyloid PET in clinical practice: Its place in the multidimensional space of Alzheimer's disease. Neuroimage Clin 2013;2:497-511.
10. Wang YT, Edison P. Tau imaging in neurodegenerative diseases using positron emission tomography. Curr Neurol Neurosci Rep 2019;19:45.
11. Harada R, Okamura N, Furumoto S, Furukawa K, Ishiki A, Tomita N, et al. 18F-THK5351: A novel PET radiotracer for imaging neurofibrillary pathology in Alzheimer disease. J Nucl Med 2016;57:208-14.
12. Kovacs GG. Invited review: Neuropathology of tauopathies: principles and practice. Neuropathol Appl Neurobiol 2015;41:3-23.
13. Tzourio-Mazoyer N, Landeau B, Papathanassiou D, Crivello F, Etard O, Delcroix N, et al. Automated anatomical labeling of activations in SPM using a macroscopic anatomical parcellation of the MNI MRI single-subject brain. Neuroimage 2002;15:273-89.
14. Collins DL, Zijdenbos AP, Kollokian V, Sled JG, Kabani NJ, Holmes CJ, et al. Design and construction of a realistic digital brain phantom. IEEE Trans Med Imaging 1998;17:463-8.
15. Altomare D, Caprioglio C, Assal F, Allali G, Mendes A, Ribaldi F, et al. Diagnostic value of amyloid-PET and tau-PET: a head-to-head comparison. Eur J Nucl Med Mol Imaging 2021;48:2200-11.